Cell Host & Microbe
Article

# Proximity to PML Nuclear Bodies Regulates HIV-1 Latency in CD4+ T Cells

Marina Lusic,[1,2,*] Bruna Marini,[1,3] Hashim Ali,[1] Bojana Lucic,[1] Roberto Luzzati,[4] and Mauro Giacca[1,5,*]
[1]Molecular Medicine Laboratory, International Centre for Genetic Engineering and Biotechnology (ICGEB), 34149 Trieste, Italy
[2]AIDS Immunopathogenesis Unit, Division of Immunology, Transplantation, and Infectious Diseases, San Raffaele Scientific Institute, 20132 Milano, Italy
[3]Scuola Normale Superiore, 56126 Pisa, Italy
[4]Struttura Complessa Malattie Infettive, Azienda Ospedaliero-Universitaria, 34100 Trieste, Italy
[5]Department of Medical, Surgical and Health Sciences, University of Trieste, 34100 Trieste, Italy
*Correspondence: lusic@icgeb.org (M.L.), giacca@icgeb.org (M.G.)
http://dx.doi.org/10.1016/j.chom.2013.05.006

## SUMMARY

**Nuclear bodies (NBs), characterized by the presence of the promyelocytic leukemia (PML) protein, are important components of the nuclear architecture, contributing to genetic and epigenetic control of gene expression. In investigating the mechanisms mediating HIV-1 latency, we determined that silenced but transcriptionally competent HIV-1 proviruses reside in close proximity to PML NBs and that this association inhibits HIV-1 gene expression. PML binds to the latent HIV-1 promoter, which coincides with transcriptionally inactive facultative heterochromatic marks, notably H3K9me2, at the viral genome. PML degradation and NB disruption result in strong activation of viral transcription as well as release of G9a, the major methyltransferase responsible for H3K9me2, and loss of facultative heterochromatin marks from the proviral DNA. Additionally, HIV-1 transcriptional activation requires proviral displacement from PML NBs by active nuclear actin polymerization. Thus, nuclear topology and active gene movement mediate HIV-1 transcriptional regulation and have implications for controlling HIV-1 latency and eradication.**

## INTRODUCTION

Functional compartmentalization of the eukaryotic cell nucleus has implications for all aspects of genome function. In particular, gene localization within specialized nuclear compartments essentially regulates gene expression (Takizawa et al., 2008; Zhao et al., 2009). Active genes tend to localize within the nuclear interior but can also associate with nuclear speckles or the nuclear pore complex. Other nuclear neighborhoods, such as the nuclear membrane/lamina, and the perinucleolar chromatin are associated with transcriptionally silent loci or gene-poor chromosomal regions (Brown et al., 1997; Finlan et al., 2008). An important feature of these associations between various loci and subnuclear domains is that they are dynamic and can change in response to cellular signals.

One prominent nuclear structure, known as the promyelocytic leukemia (PML) nuclear body (NB), has been diversely associated to a number of cellular functions, ranging from cellular protein modification to antiviral defense (reviewed in Bernardi and Pandolfi, 2007; Lallemand-Breitenbach and de Thé, 2010). This compartment is characterized by the prominent localization of the PML protein (also known as Trim19), which belongs to the large family of Tripartite motif (TRIM) proteins, the members of which display antiretroviral properties (Nisole et al., 2005). The PML protein partitions between the nucleoplasmic fraction and the nuclear matrix-associated PML NBs (Bernardi and Pandolfi, 2007; Lallemand-Breitenbach and de Thé, 2010). These are complex structures, rich in more than 200 cellular proteins besides PML itself (Van Damme et al., 2010), which are regulated by various cellular stresses, including viral infection, DNA damage, cell transformation, and oxidative stress (Bernardi and Pandolfi, 2007). Specific DNA regions are known to localize in close proximity to PML NBs. In human primary fibroblasts, these compartments were reported to associate with the MHC/Oct3-4 gene cluster in chromosome 6 and proposed to modulate the chromatin architecture and transcription of this gene group (Kumar et al., 2007; Shiels et al., 2001). Cellular infection with different viruses is known to profoundly modify PML NB number, distribution, and content; in addition, the genomes of certain DNA viruses are known to accumulate at the periphery of PML NBs during infection of quiescent cells (Bernardi and Pandolfi, 2007; Everett et al., 2007; Lallemand-Breitenbach and de Thé, 2010).

Despite these associations with specific cellular and viral DNA sequences, PML NBs are usually considered as nuclear structures devoid of DNA. Considering that the PML protein associates with the nuclear matrix, it is plausible that PML NBs serve to anchor and regulate various nuclear functions, including DNA replication and transcription, by controlling the chromatin architecture of the associated DNA sequences (Kumar et al., 2007).

HIV-1 efficiently infects metabolically active CD4+ T cells, in particular activated T-lymphocytes and macrophages (Manganaro et al., 2010). In these cells, including primary CD4+ T lymphocytes from HIV-1-infected patients, integration into the host cell DNA preferentially occurs in correspondence to actively transcribed genes. Once CD4+ T-lymphocytes revert to a resting, memory state, HIV-1 undergoes reversible transcriptional

silencing (Siliciano and Greene, 2011). Latently infected cells represent a major source of HIV-1 reservoirs, since these cells, not expressing any viral protein, are refractory to the current antiretroviral therapies, which only target the replicative fraction of the virus. Understanding the mechanisms regulating viral latency and reactivation, therefore, appears of paramount importance for the development of novel antiviral therapies aimed at HIV-1 eradication.

Transcription of the integrated HIV-1 virus is driven by the 5′ long terminal repeat (LTR) promoter that contains binding sites for several cellular transcription factors. Over the past years, we have extensively investigated protein-DNA interactions at the proviral DNA and discovered that most transcription factors are effectively bound to their target sites in both the latent and the activated states (Della Chiara et al., 2011; Lusic et al., 2003). What distinguishes these states, however, is the epigenetic regulation of chromatin conformation. Chromatin immunoprecipitation (ChIP) experiments have indeed demonstrated that modification of chromatin in proximity of the HIV-1 transcription start site precedes the onset of polymerase (Pol II)-driven transcription and is essential for viral gene expression to occur (Lusic et al., 2003). The actual molecular mechanisms that restrict HIV-1 gene expression in resting cells and determine latency, however, have remained largely elusive. An intriguing possibility is that the regulation of HIV-1 transcription might correlate with nuclear topology and thus depend on the localization of the proviral DNA inside the nucleus of the infected cells.

Here, by immuno-3D-fluorescent in situ hybridization (immuno-FISH), we report that, in the nucleus of latent CD4+ T cells, the HIV-1 provirus associates with the PML NB environment and that this interaction inhibits HIV-1 gene expression. Repression is mediated by anchoring, onto the viral DNA, the histone methyltransferase G9a, which induces bimethylation of histone 3 lysine 9 and the formation of facultative heterochromatin. During transcriptional reactivation, HIV-1 repositions its genome away from PML NBs through an active movement requiring nuclear actin polymerization.

## RESULTS

### The HIV-1 Provirus Resides in Close Proximity to PML Nuclear Bodies in Latent J-Lat Jurkat Cell Clones

We explored the spatial relationship between the HIV-1 provirus and PML NBs by 3D-FISH combined with immunostaining. A first set of experiments was performed in three clones of chronically infected Jurkat CD4+ T cells (J-Lat 9.2, J-Lat 6.3, and J-Lat 8.4; Jordan et al., 2003). These clones harbor a full-length HIV provirus with the GFP gene replacing the viral *nef* gene and represent a bona fide cellular model for HIV-1 latency. In these clones, the distance between the provirus and the nearest PML body was determined by 3D immuno-DNA FISH, performed according to a method that preserves the 3D structure of the nucleus (Solovei and Cremer, 2010). The proviral DNA and PML were labeled by hybridization with a FITC-labeled probe and by a Cy5-conjugated antibody, respectively. Representative, single confocal images for clone J-Lat 9.2, obtained in unstimulated conditions or after 5 and 48 hr of TPA treatment, are shown in Figure 1A (HIV-1 colored in green and PML in red).

After 3D reconstruction of these confocal images, the center-to-center distance between the provirus and its closest PML NB was measured in at least 100 cells. The results showed the progressive displacement of the HIV-1 provirus from the PML NBs over time upon TPA treatment. The distances were then normalized to the nuclear diameter, and the distribution was represented by box plot analysis (Figure 1B). Statistical analysis confirmed that there was a significant difference in the observed displacements ($p < 0.001$ for both analyzed time points compared to untreated cells).

Next, we sought to determine whether the histone deacetylase (HDAC) inhibitor suberoylanilide hydroxamic acid (SAHA or vorinostat) also affected the spatial distribution of PML NB and HIV-1 provirus. SAHA is a class I HDAC inhibitor, shown to induce HIV promoter expression in vitro (Archin et al., 2009; Contreras et al., 2009), as well as in vivo and ex vivo (Archin et al., 2012). The J-Lat 9.2 clone treated with 1 μM SAHA for 48 hr was used to assess the distances between the HIV-1 provirus and the closest PML NB. The measured distances, normalized to the nuclear diameter, increased significantly with respect to the control cells ($p > 0.001$) (representative, single confocal images in Figure 1A and quantification in Figure 1B). The total number of PML bodies (see Figure S1A online) and the total levels of PML protein (cf. later, Figure 3A) did not change upon TPA or SAHA treatments.

A similar analysis, performed in J-Lat clone 6.3, showed a remarkable colocalization of the provirus with PML NB in unstimulated cells, which was progressively lost upon TPA treatment (Figure 1C). Statistical analysis of the distribution of measurements again indicated high significance of the detected differences ($p < 0.001$ for both time points; Figure 1D).

Finally, analogous findings were also obtained for clone J-Lat 8.4. Also in this case, the vast majority of integrated HIV-1 colocalized with PML NB in resting conditions, while it detached from it upon cell treatment with TPA (Figures S1C and S1D).

As a control, we used a region of the MHC class I locus of chromosome 6, which was shown to associate with PML NBs (Wang et al., 2004), and with a specific BAC that maps to this region, we confirmed the tight association between PML territories and MHC I in the J-Lat clone 9.2 (Figure S1E). Similar to what was observed for HIV-1, the distance between this locus and the closest PML body increased upon stimulation with TPA ($p < 0.001$; Figure S1F).

Taken together, these results indicate that transcriptional silencing of integrated HIV-1 occurs when it is positioned in close proximity to PML NBs in different clones of latently infected Jurkat cells.

### Latent HIV-1 Is Found in Close Proximity of PML Nuclear Bodies in Primary CD4+ T Cells

We wanted to verify whether the dynamic relationship between PML NBs and integrated HIV-1 also occurred in primary, infected CD4+ T cells. For this purpose, we took advantage of a recently developed primary cell model of latency, in which primary human CD4+ cells generate ex vivo a large number of cells latently infected with HIV-1 (Bosque and Planelles, 2011). Peripheral blood naive CD4+ T lymphocytes from normal donors ($n = 6$) were stimulated with anti-CD3/CD28 beads and cultured first in the presence of TGF-β, IL-4, and IL-12 and later IL-2. The cells

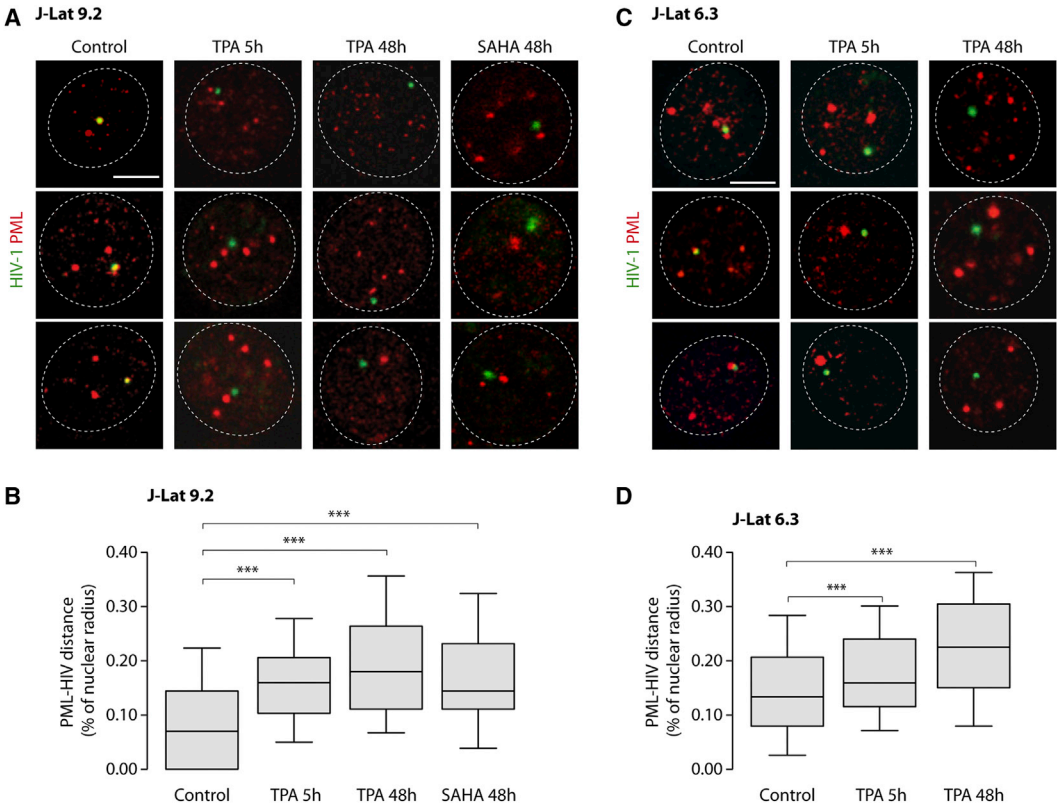


**Figure 1. HIV-1 Provirus Resides in Close Proximity of PML Nuclear Bodies in J-Lat 9.2 and 6.3 Latent Cell Clones**

(A) Representative images of 3D immuno-DNA FISH of control, TPA-treated (5 or 48 hr), and SAHA-treated (48 hr) J-Lat 9.2 cells. HIV-1 genome, green; PML, red.

(B) Box plot graphs showing the distribution of 3D measurements of the minimum separation distance between the integrated latent provirus and the closest PML NB, normalized for the nuclear diameter (n = 100 cells). ***$p < 0.001$.

(C and D) (C) As in (A), except for the SAHA treatment. (D) As in (B) for the J-Lat 6.3 clone.

Related to Figure S1.

were then infected at a low moi (0.5–0.75 μg p24/1 × $10^6$ cells) with HIV-1 obtained from the Env- molecular clone pNL4-3/$E^-R^-$, which performs a single-round infection once pseudotyped with VSV-G (Connor et al., 1995). The infected cells were kept in culture for 12–13 days to enter a resting state, after which they were reactivated by restimulation with anti-CD3/CD28 beads (Figure 2A). The levels of HIV-1 gene expression increased over 50 times when the resting cells were reactivated (Figure 2B).

3D immuno-DNA FISH for proviral DNA and PML was performed in the two conditions, with representative images for latent and reactivated cells shown in Figure 2C and Figure 2D, respectively. Measurements were performed on >150 cells from three different donors, and in agreement with J-Lat clones we again observed that the provirus resided in close proximity of the PML NB in the latent state. The displacement of HIV-1 from the closest PML NB after reactivation showed high statistical significance ($p < 0.001$; Figure 2E).

These data obtained in latent, primary CD4+ T cells confirmed that the silent HIV-1 provirus resides in close proximity to PML NBs and that, during transcriptional reactivation, displacement of the viral genome from these subnuclear structures occurs.

## PML Knockdown Releases a Block in HIV-1 Transcription

Our FISH data raised the possibility that PML bodies impose a block that restricts viral transcription. To address this issue, we induced the downregulation of endogenous PML by two approaches: treatment with arsenic trioxide and shRNA-mediated knockdown.

Recent evidence indicates that arsenic targets the wild-type PML protein directly, by binding to the cysteine residues in zinc fingers located within the RBCC domain (Zhang et al., 2010). The treatment of J-Lat clones 9.2 and 6.3 by 1 μM arsenic trioxide for 24 hr markedly reduced the levels of PML protein, while TPA left them unaffected (Figure 3A); this concentration of arsenic did not decrease cell viability (Figure S2A). The effect of PML degradation on HIV-1 gene expression was monitored by analyzing the levels of GFP fluorescence by flow cytometry. As shown in Figure 3B for clone J-Lat 9.2 and in Figures S2C and S2D for J-Lat 6.3 and J-Lat 8.4, respectively, arsenic caused massive activation of GFP expression, with the number of GFP-positive cells raising from 5%–7% in the untreated cells to over 60%–80% in the different analyzed clones. In the same clones, the levels of HIV-1 transcripts, analyzed by real-time PCR, increased dramatically

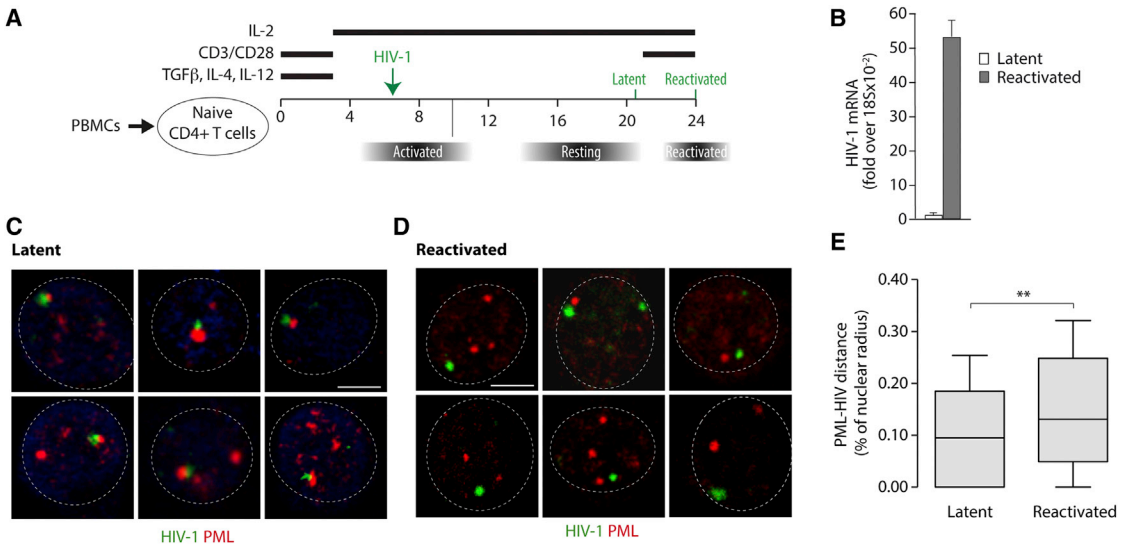


**Figure 2. PML NBs Are Associated with Latent HIV-1 Provirus in Primary CD4⁺ T Cells**

(A) Schematic representation of the experimental protocol used for the generation of latently infected human primary CD4⁺ T cells and their reactivation.

(B) Levels of HIV-1 mRNA in latently infected and reactivated CD4⁺ primary cells, determined by real-time RT-PCR. Data are represented as mean ± SEM, $p < 0.001$.

(C and D) Representative images of 3D immuno-DNA FISH of latent (n = 150) and reactivated, infected primary CD4⁺ T cells (n = 120). HIV-1 genome, green; PML, red.

(E) Distribution of 3D measurements of the minimum separation distance between the integrated latent provirus and the closest PML NB, normalized for the nuclear diameter. **$p < 0.01$.

upon arsenic treatment (>30-fold increase in clones J-Lat 8.4 and J-Lat 9.2; Figure 3C).

Next, we stably transduced the J-Lat clones 9.2 and 6.3 with a lentiviral vector expressing the puromycin-resistance gene and containing an shRNA that targets all PML isoforms (Kuroki et al., 2009), and we selected puromycin-resistant clones. PML knockdown in transduced clones was verified by both western blotting (Figure 3D) and immunofluorescence using an antibody against PML (data not shown). Remarkably, more than 90% of the transduced cells were found to have reactivated the HIV-1 LTR-driven GFP expression, as detected by flow cytometry (Figure 3E). The levels of HIV-1 mRNA upon knockdown of PML were found to be dramatically upregulated (>200- and > 300-fold increase for the J-Lat 9.2 and 6.3 clones, respectively). These levels were comparable to those obtained upon stimulation of the parental cells with 5 hr TPA treatment (Figure 3F). As a control for these experiments, we used a nontargeting lentiviral vector and an empty lentiviral vector; no changes in PML protein levels—nor in HIV-1 transcription—were observed with these controls.

To understand whether reactivation of HIV-1 gene expression upon PML knockdown was a consequence of a broader reactivation of cellular gene transcription, we analyzed, by deep sequencing, the transcriptome in the PML knockdown J-Lat 9.2 clone (PMLi) and compared the results obtained with the transcriptome from control and TPA-treated JLat 9.2 cells (Figure S2E). Despite the strong upregulation of viral transcription imparted by both anti-PML RNAi and TPA, correlation between the transcript levels was poor between these two kinds of treatments (Figure S2F), and the transcriptome of the PMLi cells was more similar to that of the untreated cells than to that of cells treated with TPA (Figure S2G). In particular, PML depletion from the cells did not activate any of the signaling pathways that are otherwise activated by TPA in lymphoid cells (Figure S2H). These results strengthen the conclusion that the repressive effect of PML on HIV-1 transcription is rather specific.

Finally, we examined the effect of PML removal by arsenic treatment in primary, latently infected CD4+ T cells. At 14 days after infection with HIV-1 pNL4-3/E⁻R⁻, a time point when the cells are in the resting phase and viral gene expression is silenced (cf. Figure 2B), arsenic trioxide 1 μM was added to the cell culture. This treatment significantly reduced the levels of endogenous PML (Figure 3G), paralleled by a massive increase in viral gene expression (>60-fold over mRNA extracted from untreated, latent cells; Figure 3H).

## PML Binds the Latent Provirus Chromatin Modified with H3K9me2, a Facultative Heterochromatin Mark

Next, we probed the association of PML with the HIV-1 genomic sequences by ChIP, using primers spanning the LTR promoter (PPR1), the region immediately downstream the transcription start site corresponding to the position of nucleosome-1 (Nuc1A), the provirus sequence (JLatA, which corresponds to the 5′ end of the *gag* gene; JLatB; and JLatC) and a control region on chromosome 19 (B13; Figure 4A). We prepared chromatin from J-Lat 9.2 cells treated with TPA or with the solvent control and immunoprecipitated it with antibodies against PML. Real-time PCR analysis of the immunoprecipitated material showed that PML was present at both the silent viral

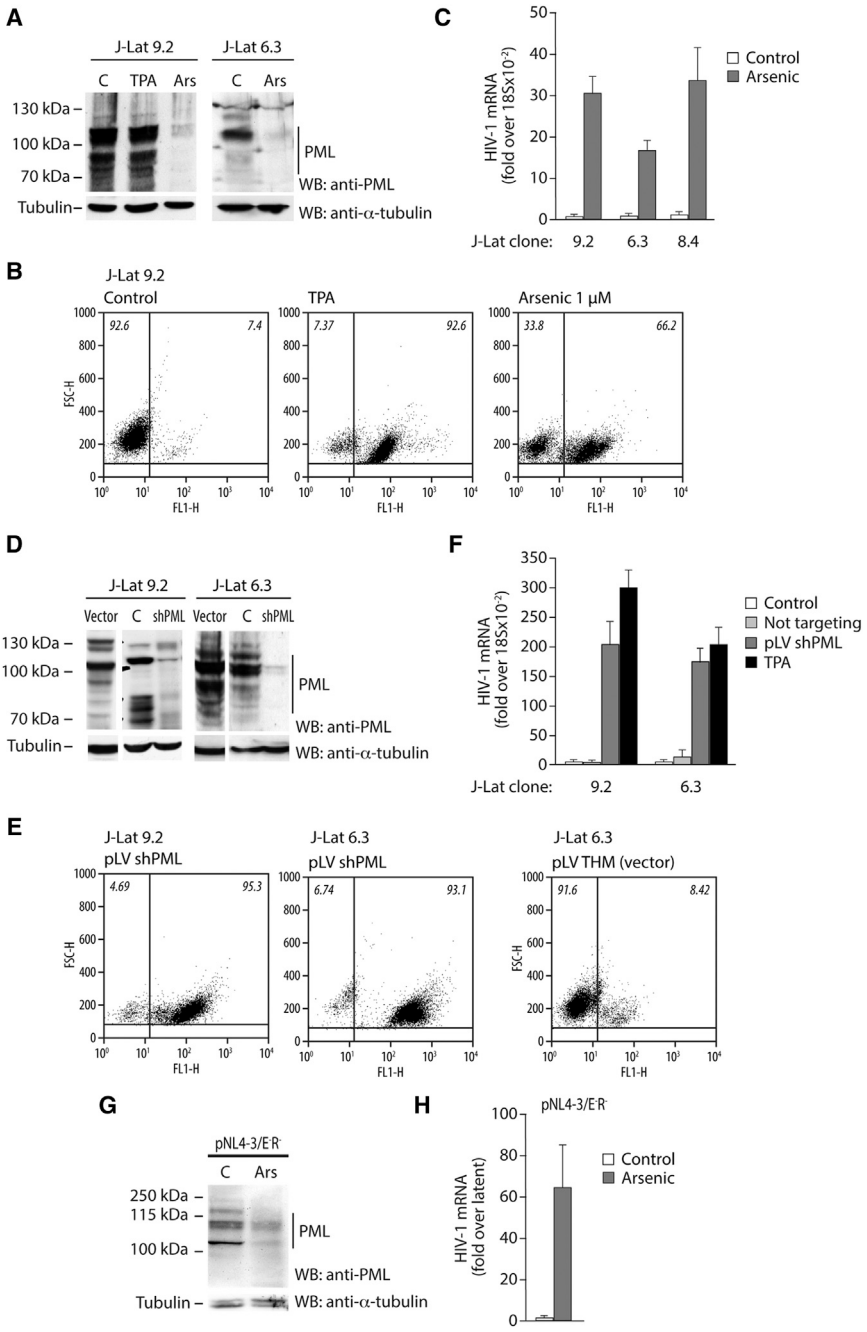


**Figure 3. HIV-1 Transcription Is Reactivated upon PML Removal**

(A) PML protein levels in whole-cell lysates of J-Lat 9.2, treated with TPA or with arsenic trioxide or J-Lat 6.3 treated with arsenic, were assessed by immunoblot for PML levels or total α-tubulin protein levels.

(B) Flow cytometry profiles of J-Lat 9.2 cells in the absence of stimulation, treated with TPA or with arsenic; the upper right gate shows GFP-positive cells. The percentage of cells in each quadrant is shown.

(C) RT-PCR measurement of HIV-1 mRNA levels in mock- or arsenic-treated J-Lat clones 9.2, 6.3, and 8.4 normalized over the 18S housekeeping gene. Data are represented as mean ± SEM. Arsenic versus control, $p < 0.001$ for all three clones.

(D) Immunoblot detection of PML protein levels, in J-Lat 9.2 or 6.3 clones stably expressing an shPML. C, parental cell clone. Vector, molecular clones obtained by transduction of the pLKO-nt, in case of the 9.2 clone or pLV THM empty vector, for clone 6.3.

(E) Flow cytometry for GFP fluorescence in J-Lat clones stably transduced with the indicated vectors.

(F) Levels of HIV-1 mRNA, determined by real-time RT-PCR, in the J-Lat clones stably transduced with the indicated vectors, or in parental cells treated with TPA (5 hr). Data are represented as mean ± SEM. P, not significant between control and not targeting; $p < 0.001$ between either pLV-shPML or TPA and control.

(G and H) Levels of PML protein (G) and of HIV-1 mRNA (H) in latently infected primary CD4+ T cells treated with arsenic. In (H), data are represented as mean ± SEM, $p < 0.001$ between control and arsenic.

Related to Figure S2.

promoter and the downstream regions; binding was abolished from all the viral sequences upon TPA stimulation (Figure 4B). Similar results were also obtained with J-Lat clone 6.3 (Figures S3A–S3C). We also probed, in the J-Lat 9.2 clone, the possible binding to the viral genome of Daxx and Sp100 proteins, two constitutive components of the PML NBs (Tavalai and Stamminger, 2008). These ChIP experiments revealed marginal binding of Sp100, irrespective of TPA treatment, and no binding of Daxx (Figures S3D–S3F).

To characterize the chromatin signatures present concomitant with PML at the silent and activated HIV-1 provirus, we immunoprecipitated chromatin with antibodies recognizing different chromatin methyl marks. The pattern of distribution of H3K9me2, a marker of facultative heterochromatin within euchromatic regions (Trojer and Reinberg, 2007), paralleled that of PML, in particular being enriched in latent cells and depleted in activated cells from both the promoter and the downstream sequences (Figure 4C). In contrast, the pattern of binding of H3K4me3 (labeling actively transcribed euchromatin) was somewhat opposed to those of PML and H3K9me2, becoming remarkably high upon TPA treatment (Figure 4D).

TPA treatment also determined the release of PML from the cellular *IL-2* gene, which was previously shown to interact with this factor (Lo et al., 2008; Nayak et al., 2009; Figure S3G). This treatment also determined a decrease in H3K9me2 marking at both the *IL-2* promoter and coding regions (Figure S3H). Of interest, while TPA determined a strong increase in *IL-2* transcription, the effects of the stable PML knockdown were more modest (Figure S3I).

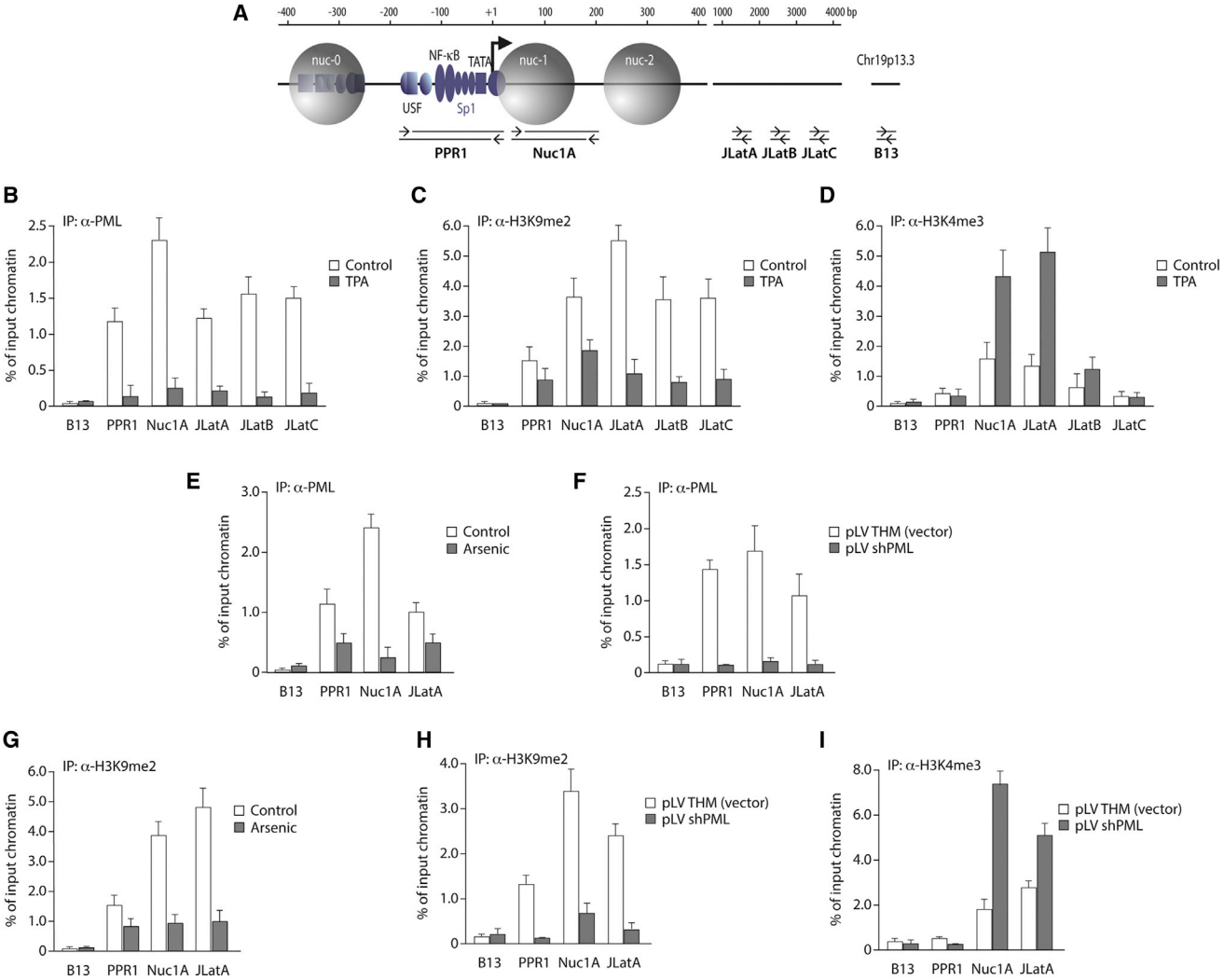


**Figure 4. PML Protein Binds the Latent Provirus Chromatin Marked with H3K9met2, a Facultative Heterochromatin Mark**

(A) Primer position along the HIV-1 sequence, with the indication of the transcription factor binding sites and the nucleosomal arrangement in correspondence to promoter and transcription start site. B13 refers to a control, genomic region mapping to chromosome 19p13.3.

(B–D) ChIP analysis of the chromatin preparations from control and TPA-treated J-Lat 9.2 using anti-PML (B), -H3K9met2 (C), -H3K4met3 (D) antibodies. $p < 0.01$ for TPA-treated versus control for all the investigated HIV-1 regions except PPR1 in all panels and JLatB and JLatC in (D).

(E and F) ChIP with anti-PML antibody in control and arsenic-treated J-Lat 9.2 cells (E) or after stable knockdown of PML by shPML lentiviral vector (F), using pLV THM-transduced cells as a control. $p < 0.01$ for arsenic-treated or shPML-treated versus control for all the investigated HIV-1 regions.

(G and H) Same as (E) and (F) using an anti-H3K9met2 antibody.

(I) Same as (F) and (H) using anti-H3K4met3 antibodies. $p < 0.01$ for arsenic-treated or shPML-treated versus control for the Nuc1A and JlatA regions in both panels.

For each antibody, values were normalized for the input amounts of chromatin and the amount immunoprecipitated by a control, anti-IgG antibody. The mean and SEM values from at least three independent samples are shown for each primer set.

Related to Figure S3.

## Chromatin Signatures at the Viral Genome Change upon PML Removal

We also wanted to study the same chromatin modifications in J-Lat clone 9.2 upon arsenic treatment or PML knockdown. In these settings, no proviral DNA sequences could be immunoprecipitated with anti-PML antibody (Figures 4E and 4F). Concomitant with a marked increase in proviral gene expression (cf. Figure 3C), a substantial loss of the repressive chromatin mark H3K9me2 at the viral Nuc1A and JLatA sequences was observed in arsenic-treated cells (Figure 5G) or in cells expressing anti-PML shRNA (Figure 5H). In contrast, PML removal determined a considerable increase in the levels of H3K4me3 at viral sequences downstream of the nucleosome-free region, amplified with PPR1 and JLatA primers (Figure 5I).

SAHA treatment (1 μM for 48 hr), despite causing only a modest increase in HIV-1 mRNA levels (Figure S3J) compared

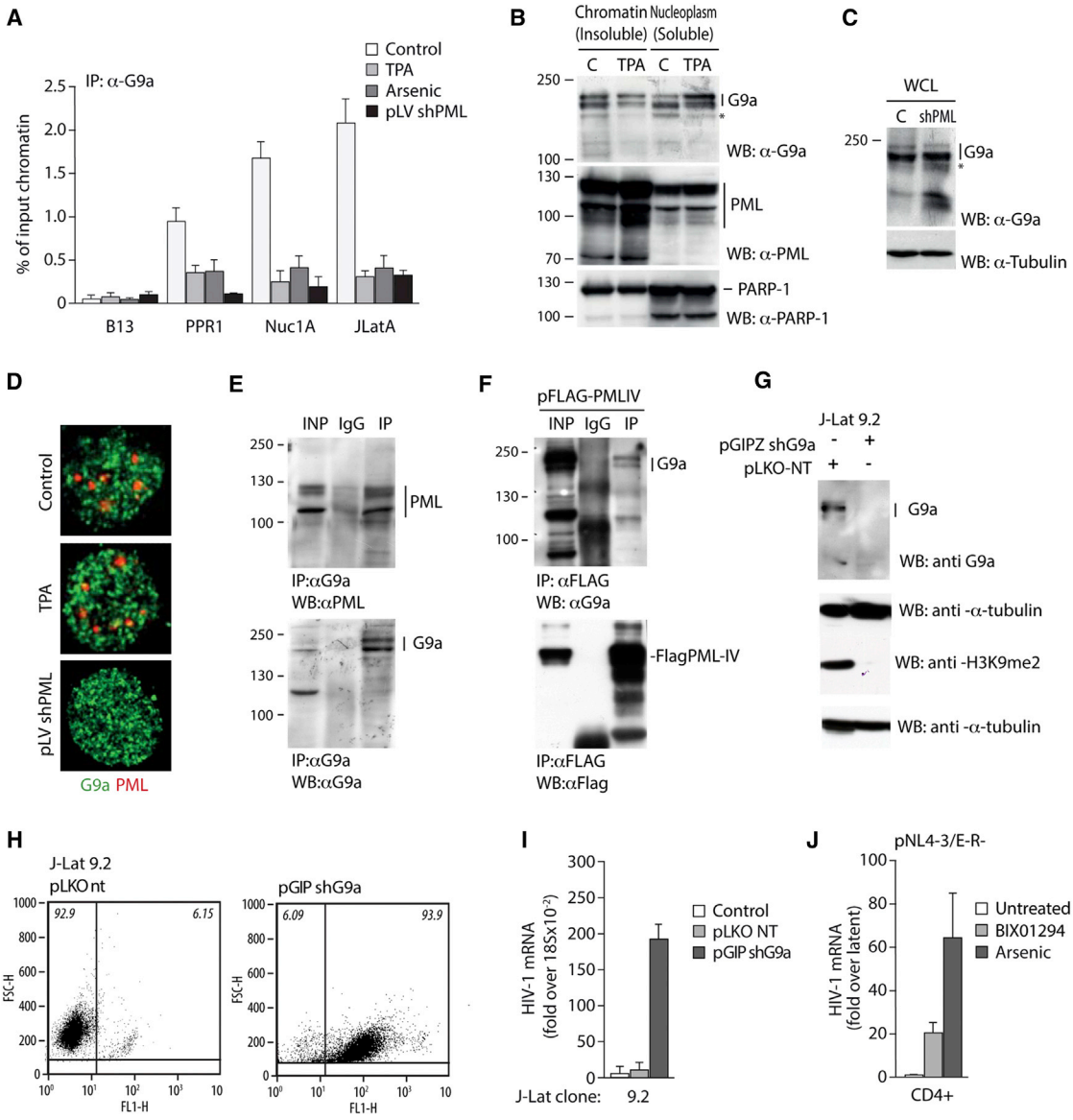


**Figure 5. G9a Methyltransferase Requires PML Protein to Bind the Viral Genome**

(A) ChIP with G9a antibody in control J-Lat 9.2 cells, untreated or treated with TPA or arsenic, or transduced with pLVshPML. Data are represented as mean ± SEM, $p < 0.001$ between control and all treated samples.

(B) G9a and PML protein levels in insoluble and soluble nuclear fractions of control and TPA-treated cells. PARP-1protein served as a loading control. Asterisk stands for the unspecific band.

(C) Immunoblot for G9a in whole-cell lysates (WCL) from control or shPML-expressing cells; tubulin served as a loading control.

(D) Immunofluorescence for G9a (green) and PML (red) in control, TPA-treated, or pLV shPML-transduced cells.

(E) Immunoblot for PML (upper panel) or G9a (lower panel) of G9a immunoprecipitated J-Lat 9.2 nuclear extracts.

(F) Immunoblot for G9a (upper panel) or Flag (lower panel) of Flag-immunoprecipitated HEK293 cells transfected with Flag-PML IV.

(G) Immunoblot for G9a and H3K9me2 in J-Lat 9.2 clones stably transduced with pLKO-NT or pGIP-Z shG9a lentiviral constructs.

(H) Flow cytometry profiles of J-Lat 9.2 cells transduced with indicated vectors.

(I) HIV mRNA levels in the same cells. Data are represented as mean ± SEM, $p < 0.001$ between either control and the shG9a-treated sample.

(J) HIV mRNA levels in primary latent CD4+ cells treated with indicated drugs. Data are represented as mean ± SEM, $p < 0.05$ between arsenic- and BIX-1294-treated cells.

Related to Figure S4.

to TPA (cf. Figure 3G), markedly decreased PML-provirus binding and determined a loss of the H3K9me2 mark (Figures S3K and S3L).

Together, these results suggest that binding of PML with the provirus correlates strictly with the presence of chromatin marks suppressive of gene expression.

### PML-Dependent Binding of H3K9 Dimethyltransferase G9a to the Viral Genome

Since the H3K9me2 mark was significantly decreased on the viral DNA sequences upon PML knockdown, we tested whether the PML protein might mediate association of G9a, the major methyltransferase responsible for H3K9 dimethylation (Rice et al., 2003), to the provirus. We immunoprecipitated chromatin from the J-Lat clone 9.2 with a specific G9a antibody, and we observed binding of this histone methyltransferase to the viral sequences in unstimulated cells (Figure 5A). Activation of the viral promoter with either TPA, arsenic, or SAHA, all of which decreased H3K9met2, coincided with a strong depletion of G9a from the provirus (Figure 5A and Figure S4). Similarly, knockdown of PML using the pLV shPML lentiviral vector also caused a decrease in provirus-bound G9a. The total levels of G9a protein in the nuclear fraction did not show any significant changes upon induction of the cells with TPA (Figure 5B); neither did they change upon PML knockdown, as shown by immunoblotting (Figure 5C) and immunofluorescence (Figure 5D). We then assessed the direct binding between PML and G9a, by immunoprecipitating endogenous G9a protein from the J-Lat 9.2 nuclear extracts followed by immunoblotting for PML (Figure 5E). This interaction was confirmed on exogenously expressed Flag-PML-IV isoform that coimmunoprecipitated G9a in HEK293 cells.

Next we stably transduced the J-Lat clone 9.2 with pGZIP-G9a lentiviral vector, selected stable clones, and controlled the efficiency of knockdown by immunoblotting with anti-G9a and anti-H3K9me2 (Figure 5G). Remarkably, more than 90% of the transduced cells reactivated GFP expression, as detected by flow cytometry (Figure 5H). The levels of HIV-1 mRNA upon G9a knockdown increased sharply, as compared to control cells transduced with a pLKO-nontargeting lentiviral vector (>200-fold) (Figure 5I). Finally, the effect of G9a inhibition in primary, latently infected CD4+ cells was examined by adding the specific G9a inhibitor BIX01294 (Imai et al., 2010) to the cell culture. This treatment markedly activated viral gene expression (>20-fold), even if not as strong as arsenic (>60-fold; Figure 5J).

### Displacement of the HIV-1 Provirus from PML NBs Is Necessary for Viral Transcriptional Activation

Our FISH and ChIP results demonstrate that HIV-1, when transcriptionally silent, colocalizes with PML NBs and that activation of transcription results in repositioning of the provirus away from the PML-rich neighborhood. In a growing number of cases, repositioning of specific cellular genomic sequences to different regions of the nucleus requires active nuclear actin polymerization (Skarp and Vartiainen, 2010). We therefore wanted to test the possibility that nuclear actin might also be involved in HIV-1 transcriptional activation. J-Lat 9.2 cells were treated for 1.5 hr with cytochalasin D (CytD), a powerful inhibitor of actin polymerization, before activation with TPA for additional 5 hr. Alternatively, we first treated the cells with TPA for 5 hr, followed by 1.5 hr treatment with CytD. We found that addition of the actin polymerization inhibitor before treatment with TPA significantly inhibited HIV-1 transcription (>5-fold reduction); in contrast, when HIV-1 transcription was induced before actin depolymerization, no significant decrease in levels of HIV-1 transcripts was detected (Figure 6A).

To prove that the inhibition of actin polymerization influences repositioning of the viral genome from the closest PML NBs, thus impeding the transcriptional activation of the virus, we analyzed the spatial relationship of the HIV-1 DNA and PML by 3D immuno-DNA FISH on J-Lat 9.2 cells treated first with CytD and then with TPA. We measured the distances between the provirus and its closest PML NB in 100 cells (representative images are shown in Figure 6B) and normalized these values to the nuclear diameter. We found that inhibition of actin polymerization blocked displacement of the provirus from the PML NBs upon TPA treatment ($p < 0.001$; Figure 6C).

Finally, we assessed the binding of nuclear actin to the viral genome by ChIP. Upon TPA treatment and concomitant with the induction of viral transcription, nuclear actin binding to the viral promoter and to the provirus body was greatly enhanced (Figure 6D). The levels of actin binding to the viral genome were inversely correlated with those of PML (Figure 6E). However, when cells were treated with CytD prior to TPA, PML protein remained bound to the viral genome, together with H3K9met2 and G9a methyltransferase (Figures 6F and 6G, respectively).

Taken together, these results indicate that transcriptional activation of the silent HIV-1 is coupled with repositioning of the provirus from PML NBs and that the inhibition of actin polymerization impedes both events.

## DISCUSSION

A major finding reported in this manuscript is that nuclear topology essentially regulates HIV-1 gene expression and, in particular, latency and reactivation. In latently infected T cell lines and primary CD4+ T cells, the HIV-1 provirus is found associated with the PML protein, as detected by both immuno-FISH and ChIP. This interaction negatively regulates transcription by mediating association of the provirus with the G9a methyltransferase, which modifies the HIV-1 chromatin by the H3K9me2 suppressive chromatin mark. Transcriptional activation requires repositioning of the provirus away from PML NBs through a movement involving active actin polymerization.

Association of PML bodies with specific chromosomal loci was shown to be nonrandom in human and murine cells. Combined immunolocalization of PML bodies with specific in situ hybridization of cellular genomic loci has provided convincing evidence that PML associates with certain loci with higher frequency. For example, it was shown that the *TP53* gene localizes with PML NBs in approximately 50% of Jurkat cells (Sun et al., 2001), while the major histocompatibility (MHC/Oct3-4) gene cluster associates with PML NBs in human primary fibroblasts (Kumar et al., 2007; Wang et al., 2004).

While the functional significance of the colocalization of PML NBs with cellular loci remains poorly defined in most cases, a number of studies indicate that these nuclear structures play an important role in the life cycles of different, nuclear-replicating DNA viruses and of some retroviruses. In particular, parental genomes of herpes simplex type 1 (HSV-1), human cytomegalovirus (HCMV), and adenovirus associate with PML NBs, which delay or block their replication (Ahn and Hayward, 2000; Doucas et al., 1996; Everett et al., 2007). The antiviral state is often defined by the presence of Daxx and Sp100, permanent NB

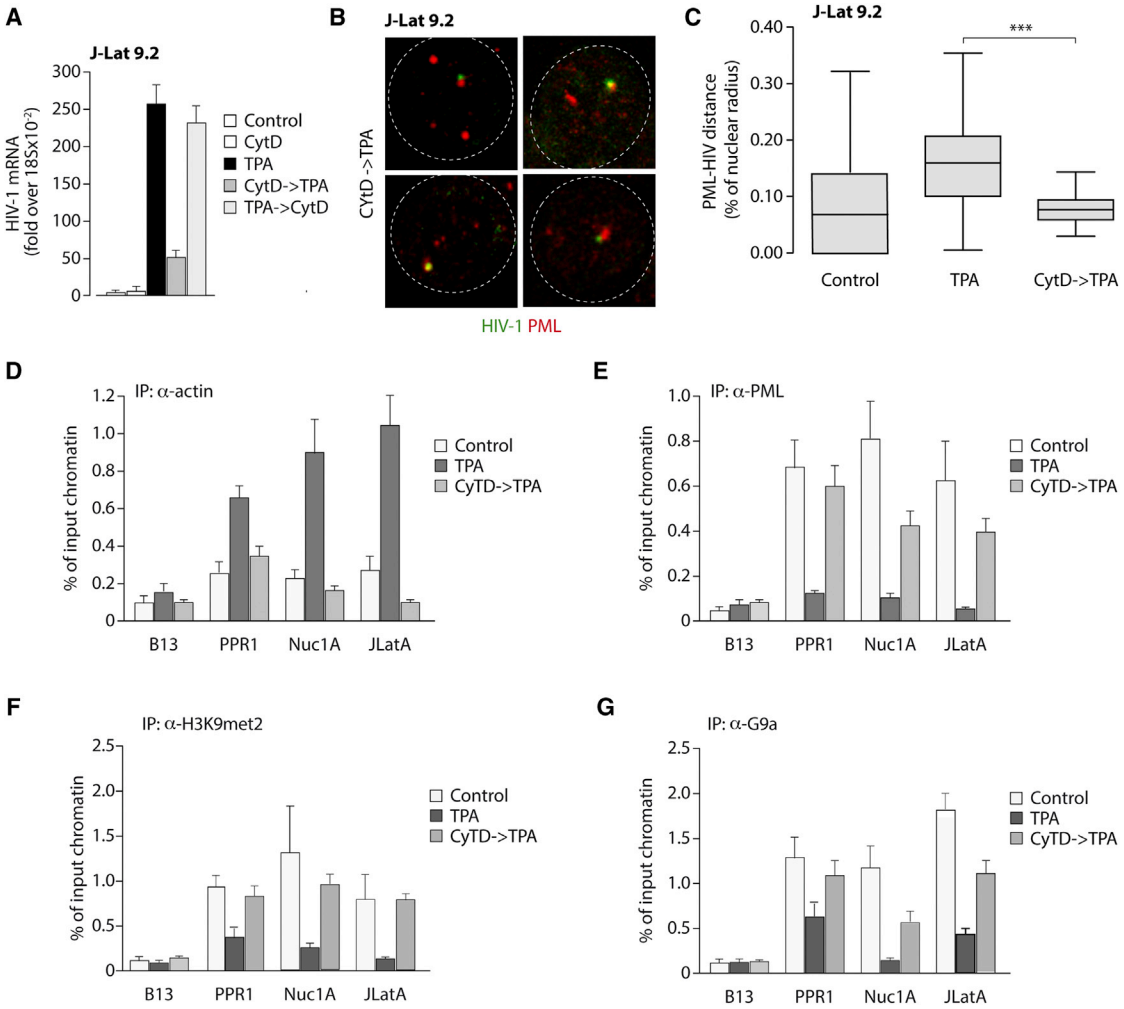


**Figure 6. HIV-1 Genome Displacement from PML NBs during Transcriptional Activation Is Mediated by Polymerization of Nuclear Actin**

(A) HIV-1 mRNA levels in J-LAT 9.2 cells treated with CytD followed by TPA (CytD→TPA), or the reverse (TPA→CytD), measured as in Figure 3. Data are represented as mean ± SEM.

(B) 3D immuno-DNA FISH images of cells treated with CytD followed by TPA. HIV-1 (green) and PML (red).

(C) Quantitative analysis of the distribution of distances (n = 100 per group). ***$p < 0.001$. The distributions of control and CytD→TPA values are not significantly different.

(D–G) ChIP analysis with anti-β actin (D), anti-PML (E), anti-H3K9me2 (F), and anti-G9a (G) antibodies in J-Lat cells treated for 4 hr with TPA, or with CytD for 2 hr prior to TPA (CytD→TPA); control are mock-treated cells. $p < 0.05$ for all the three investigated HIV-1 regions between TPA and CytD→TPA for all four investigated antibodies. Data are represented as mean ± SEM.

residents that can either cooperate with PML (Glass and Everett, 2013) or act independently (Shalginskikh et al., 2013). Our study, however, reveals a rather specific interaction of HIV-1 DNA with PML, while Daxx was not detected at the provirus and interaction with Sp100 was weak and independent of transcriptional regulation. Both PML and Sp100 are known to be induced by interferon (IFN) (Chelbi-Alix et al., 1998); since IFN signaling exerts inhibitory effects on HIV-1 replication (cf. Vendrame et al., 2009, and citations therein), an interesting possibility is that these effects might be, at least in part, exerted through PML induction.

Our results show that the spatial positioning of HIV-1 provirus essentially regulates viral transcription: a negative role of PML in viral transcription is supported by both correlative information (spatial relationship of latent HIV-1 with PML NBs and immunoprecipitation of PML together with H3K9me2-marked HIV-1 chromatin) and functional data (activation of HIV-1 transcription by disruption of PML bodies with arsenic or downregulation of PML protein by anti-PML shRNA). PML has been shown to repress transcription by physically and functionally interacting with class I HDACs (Wu et al., 2001). Class I HDACs are blocked by SAHA, and treatment with this inhibitor provokes chromatin modifications and reduction of HDAC-1 occupancy at the HIV-1 promoter (Archin et al., 2009, 2012). Our results show that SAHA treatment displace the provirus from the closest PML body, thus suggesting that PML might act together with class I HDACs to repress HIV-1 transcription. In line with this possibility, our previously published work has shown that changes in the histone acetylation patterns precede the onset

of productive transcription (Lusic et al., 2003), thus suggesting that repositioning of the viral genome from the PML NB occurs before transcriptional activation of the viral promoter. The ChIP experiments indicating direct or indirect binding of PML to HIV-1 chromatin appear to be rather specific, since, under the same conditions, none of the tested control genomic regions (B13 region on chromosome 19, shown in Figure 4; region B48 of the *TIMP13* promoter, *NPLOC4* gene, and a lamin-associated region in chromosome 9p21.1, data not shown) scored positive for this association. In addition, binding was lost upon HIV-1 transcriptional activation.

A large number of transcription factors and cofactors are described to be recruited to the PML NBs or in their proximity; thus, PML NBs may be viewed as chromatin-close deposit sites for sequestration or release of factors required for transcriptional activation or repression (Van Damme et al., 2010). This notion appears compatible with the reported role of PML as a transcriptional coactivator in certain circumstances (Chuang et al., 2011; Lo et al., 2008) and corepressor in others (Seeler et al., 1998; Vallian et al., 1998). As far as the HIV-1 provirus is concerned, we have already observed that PML plays a negative role in its transcriptional regulation. In particular, we reported that the overexpression of Cyclin T1 (the cyclin component of the P-TEFb kinase, essential for HIV-1 transcription) forces localization of this protein into PML NBs and represses transcription (Marcello et al., 2003) and that a transcriptionally inactive form of CDK9, the kinase component of P-TEFb, acetylated in its catalytic domain, specifically resides inside PML NBs (Sabò et al., 2008). These results reinforce the conclusion that PML represents a nuclear neighborhood that is repressive for HIV-1 transécription.

Transcriptional silencing, as the principal feature of HIV-1 latency, can be achieved and maintained through mechanisms involving epigenetic changes of chromatin (Lusic et al., 2003). Latent HIV proviruses were shown to carry trimethylated histone H3 on either lysine 9 (H3K9met3) or lysine 27 (H3K27met3), as well as H3K9met2 (Archin et al., 2009; du Chéné et al., 2007; Imai et al., 2010). In particular, here we show that H3K9met2, a modification associated with facultative heterochromatin that labels the genes poised for transcription (Trojer and Reinberg, 2007), marks the latent HIV-1 chromatin, concomitant with its association with PML and with the major H3K9met2 methyltransferase G9a. This finding is in perfect agreement with a recent report showing that a chemical inhibitor of G9a was able to reactivate HIV-1 from latency (Imai et al., 2010). Interestingly, we found that presence of the PML protein and integrity of PML NBs were essential requisites for G9a to associate with the latent HIV-1 proviral DNA. This information is consistent with the conclusion that the interaction of G9a with the viral genome and the consequent repressive methylation of its chromatin is mediated by PML. Considering that PML has been reported to be involved in chromatin organization on certain genomic regions (Kumar et al., 2007) and genes (Chuang et al., 2011), one might hypothesize that PML contributes to chromatin organization of those genes which are poised for transcription and become rich in facultative chromatin marks.

G9a is not the only histone methyltransferase described to associate with latent HIV-1; Suv39H1 and its associating factors such as HP1 proteins were also found to accumulate in the vicinity of the latent provirus (du Chéné et al., 2007). Although we could detect H3K9me3, the major modification imparted by Suv39H1, at the silenced viral genome, we were unable to establish a clear pattern for this histone mark upon transcriptional activation (data not shown). It is, however, apparent from different studies, including this one, that heterogenous epigenetic modifications contribute to the silencing of HIV-1 in latent cells (Archin et al., 2009; du Chéné et al., 2007; Imai et al., 2010).

Reactivation of viral transcription upon induction is followed by loss of PML and G9a interaction with the viral sequences and, most significantly, by the repositioning of the provirus away from PML NBs. When we tested whether gene movements were involved in reactivation of HIV-1 transcription, by inhibiting actin polymerization, we observed that HIV-1 transcription could not be reactivated and that the virus remained closely attached to its closest PML NB. Movement of chromatin inside the nucleus is progressively being appreciated as important for the regulation of gene expression. In yeast, activated genes are repositioned to the nuclear pore complex for RNA export (Taddei et al., 2006). During transcriptional silencing, genes in lymphoid cells move near centromeric heterochromatin, whereas transcriptional activation of the *β-globin* locus involves movement of the gene away from centromeric heterochromatin (Kosak et al., 2002). *IgH* and *Igκ* loci are localized at the nuclear periphery in hematopoietic progenitors but move internally during transcriptional activation during B cell development (Brown et al., 1997). Actively transcribed genes are also brought into close contact with nuclear speckles, sites considered to be hubs of RNA metabolism (Brown et al., 2008). Thus, the HIV-1 provirus joins the probably still very partial lists of gene sequences that are essentially regulated at the transcriptional level by nuclear topology. Despite the significant number of examples connecting gene movement with changes in transcriptional activity, it is still unclear whether intranuclear movement of chromatin is the cause or result of changes in transcriptional activity. Nuclear forms of actin and myosin have been implicated in mediating long-range, directed movements (Chuang et al., 2006; Dundr et al., 2007; Miyamoto et al., 2011), while, at the same time, mounting evidence shows their role in cellular transcription, chromatin remodeling, and mRNA export (Visa and Percipalle, 2010).

Which molecular mechanisms are physically linking transcriptional activation, actin polymerization, and movement away from PML bodies, as well as the understanding of whether actin polymerization impacts on transcriptional initiation or elongation, clearly requires further investigation. In this respect, however, it appears interesting to consider that previous reports have indicated that actin directly interacts with p65/RelA of NF-κB (Are et al., 2000; Fazal et al., 2007). It is therefore tempting to speculate that this factor might bridge the HIV-1 LTR enhancer region with nuclear actin.

Finally, our findings regarding the repressive nature of PML protein and especially the strong capacity of arsenic trioxide to mediate viral transcriptional activation by inducing PML degradation might be of potential therapeutic interest. Arsenic trioxide is an ancient drug used in the Chinese traditional medicine, which exerts a substantial anticancer activity in patients with acute PML by promoting PML-RARα degradation (Zhang et al., 2010). The potential of arsenic to degrade PML can be explored

in the treatment of HIV-1 infection, as an alternative to HDAC inhibitors (Margolis, 2011), to reactivate the latent viral reservoir followed by effective antiretroviral therapy, having the ultimate aim to achieve virus eradication.

## EXPERIMENTAL PROCEDURES

### Primary Cell Isolation and Culture

Peripheral blood mononuclear cells (PBMCs), obtained from healthy blood donors after approval by the Ethical Committee of the Azienda Ospedaliero-Universitaria "Ospedali Riuniti di Trieste," Italy, were isolated as described (Manganaro et al., 2010). For the details of CD4+ purification and culture, see the Supplemental Experimental Procedures.

### Virus Production and Infection

Viral stocks were generated using the *env* molecular clone pNL4-3/$E^-R^-$, a kind gift from Dr. Nathaniel Landau. Details on virus production and infection are reported in the Supplemental Experimental Procedures.

### 3D Immuno-DNA FISH

Three-dimensional FISH and immunostaining were performed as described (Solovei and Cremer, 2010), with the modifications reported in the Supplemental Experimental Procedures.

### Chromatin Immunoprecipitation

ChIP was performed as described previously (Perkins et al., 2008), with some modifications introduced for J-Lat cells (see the Supplemental Experimental Procedures).

### Coimmunoprecipitation

Immunoprecipitations of endogenous G9a were performed using the J-Lat 9.2 nuclear extracts, whereas for exogenously expressed PML protein HEK293T cells were used (as reported in the Supplemental Experimental Procedures).

### qRT-PCR

For the quantification of HIV transcript levels, RNA was purified from the cells with the NucleoSpin RNA II purification kit (Macherey-Nagel), and the mRNA levels were quantified by TaqMan qRT-PCR by using HIV-1 primers and probes (Perkins et al., 2008) and housekeeping gene controls (GAPDH and18S rRNA).

### RNA Sequencing

For the transcriptomic analysis, total RNA was extracted from untreated 9.2 J-Lat cells, cells treated with TPA for 5 hr, and from a J-Lat 9.2-derived stable clone expressing shPML.

Deep sequencing was performed by IGA Technology Services (Udine, Italy). Samples were processed using TruSeq RNA-seq sample prep kit from Illumina (Illumina, Inc.), and CLC-Bio Genomics Workbench software (CLC Bio) was used to calculate gene expression levels (see the Supplemental Experimental Procedures for details).

### Flow Cytometry Analysis

Cell fluorescence was measured with the FACSCalibur (BD Bioscience). To phenotype CD4+ T cells, these were stained with the following mABs: FITC-conjugated anti-CD4+, PerPC-conjugated anti-CD45RA, and phycoerythrin-conjugated (PE)-anti CD45RO (Miltenyi Biotec). Flow cytometry data were analyzed with FlowJo software or Cellquest (BD Bioscience). Analysis was restricted to the live population, as defined by the forward versus side scatter profile.

### Arsenic Toxicity Test

To test the toxicity of arsenic on primary $CD4^+$ T cells and on J-Lat 9.2 cells, the cellular adenosine triphosphate (ATP) levels were measured by a luminescence assay (ATPlite, Perkin Elmer). Cells ($8 \times 10^4$) were cultured for 24 hr in medium containing different concentration of arsenic trioxide (1, 2, and 10 μM). After cell lysis, ATP concentration was measured as luminescence according to the manufacturers' protocol.

### Statistical Analysis

Statistical analysis was performed using R software (http://www.r-project.org/) and Prism 4. Statistical analysis of FISH signals was performed by applying the Mann-Whitney-Wilcoxon rank sum test. Star code for statistical significance is as follows: ***$p < 0.001$, **$p < 0.01$,*$p < 0.05$.

For the ChIP and RT-PCR results, the reported values are mean and standard error of the mean (SEM), calculated from at least three independent samples. Statistical significance was evaluated using one-way ANOVA and Bonferroni/Dunn's post hoc test.

## SUPPLEMENTAL INFORMATION

Supplemental Information includes four figures, Supplemental Experimental Procedures, and Supplemental References and can be found with this article at http://dx.doi.org/10.1016/j.chom.2013.05.006.

## ACKNOWLEDGMENTS

The authors are very grateful to Dr. Piergiorgio Percipalle for the insightful comments and suggestions. This work was supported by grants from the Italian National Research Programme on AIDS of the Istituto Superiore di Sanità, Italy to M.G. and M.L. and from the Young Investigator Grant RF2007-16 of the Italian Ministry of Health to M.L.

Received: October 10, 2012
Revised: March 5, 2013
Accepted: April 26, 2013
Published: June 12, 2013

## REFERENCES

Ahn, J.H., and Hayward, G.S. (2000). Disruption of PML-associated nuclear bodies by IE1 correlates with efficient early stages of viral gene expression and DNA replication in human cytomegalovirus infection. Virology *274*, 39–55.

Archin, N.M., Espeseth, A., Parker, D., Cheema, M., Hazuda, D., and Margolis, D.M. (2009). Expression of latent HIV induced by the potent HDAC inhibitor suberoylanilide hydroxamic acid. AIDS Res. Hum. Retroviruses *25*, 207–212.

Archin, N.M., Liberty, A.L., Kashuba, A.D., Choudhary, S.K., Kuruc, J.D., Crooks, A.M., Parker, D.C., Anderson, E.M., Kearney, M.F., Strain, M.C., et al. (2012). Administration of vorinostat disrupts HIV-1 latency in patients on antiretroviral therapy. Nature *487*, 482–485.

Are, A.F., Galkin, V.E., Pospelova, T.V., and Pinaev, G.P. (2000). The p65/RelA subunit of NF-kappaB interacts with actin-containing structures. Exp. Cell Res. *256*, 533–544.

Bernardi, R., and Pandolfi, P.P. (2007). Structure, dynamics and functions of promyelocytic leukaemia nuclear bodies. Nat. Rev. Mol. Cell Biol. *8*, 1006–1016.

Bosque, A., and Planelles, V. (2011). Studies of HIV-1 latency in an ex vivo model that uses primary central memory T cells. Methods *53*, 54–61.

Brown, K.E., Guest, S.S., Smale, S.T., Hahm, K., Merkenschlager, M., and Fisher, A.G. (1997). Association of transcriptionally silent genes with Ikaros complexes at centromeric heterochromatin. Cell *91*, 845–854.

Brown, J.M., Green, J., das Neves, R.P., Wallace, H.A., Smith, A.J., Hughes, J., Gray, N., Taylor, S., Wood, W.G., Higgs, D.R., et al. (2008). Association between active genes occurs at nuclear speckles and is modulated by chromatin environment. J. Cell Biol. *182*, 1083–1097.

Chelbi-Alix, M.K., Quignon, F., Pelicano, L., Koken, M.H., and de Thé, H. (1998). Resistance to virus infection conferred by the interferon-induced promyelocytic leukemia protein. J. Virol. *72*, 1043–1051.

Chuang, C.H., Carpenter, A.E., Fuchsova, B., Johnson, T., de Lanerolle, P., and Belmont, A.S. (2006). Long-range directional movement of an interphase chromosome site. Curr. Biol. *16*, 825–831.

Chuang, Y.S., Huang, W.H., Park, S.W., Persaud, S.D., Hung, C.H., Ho, P.C., and Wei, L.N. (2011). Promyelocytic leukemia protein in retinoic acid-induced chromatin remodeling of Oct4 gene promoter. Stem Cells *29*, 660–669.

Connor, R.I., Chen, B.K., Choe, S., and Landau, N.R. (1995). Vpr is required for efficient replication of human immunodeficiency virus type-1 in mononuclear phagocytes. Virology *206*, 935–944.

Contreras, X., Schweneker, M., Chen, C.S., McCune, J.M., Deeks, S.G., Martin, J., and Peterlin, B.M. (2009). Suberoylanilide hydroxamic acid reactivates HIV from latently infected cells. J. Biol. Chem. *284*, 6782–6789.

Della Chiara, G., Crotti, A., Liboi, E., Giacca, M., Poli, G., and Lusic, M. (2011). Negative regulation of HIV-1 transcription by a heterodimeric NF-κB1/p50 and C-terminally truncated STAT5 complex. J. Mol. Biol. *410*, 933–943.

Doucas, V., Ishov, A.M., Romo, A., Juguilon, H., Weitzman, M.D., Evans, R.M., and Maul, G.G. (1996). Adenovirus replication is coupled with the dynamic properties of the PML nuclear structure. Genes Dev. *10*, 196–207.

du Chéné, I., Basyuk, E., Lin, Y.L., Triboulet, R., Knezevich, A., Chable-Bessia, C., Mettling, C., Baillat, V., Reynes, J., Corbeau, P., et al. (2007). Suv39H1 and HP1gamma are responsible for chromatin-mediated HIV-1 transcriptional silencing and post-integration latency. EMBO J. *26*, 424–435.

Dundr, M., Ospina, J.K., Sung, M.H., John, S., Upender, M., Ried, T., Hager, G.L., and Matera, A.G. (2007). Actin-dependent intranuclear repositioning of an active gene locus in vivo. J. Cell Biol. *179*, 1095–1103.

Everett, R.D., Murray, J., Orr, A., and Preston, C.M. (2007). Herpes simplex virus type 1 genomes are associated with ND10 nuclear substructures in quiescently infected human fibroblasts. J. Virol. *81*, 10991–11004.

Fazal, F., Minhajuddin, M., Bijli, K.M., McGrath, J.L., and Rahman, A. (2007). Evidence for actin cytoskeleton-dependent and -independent pathways for RelA/p65 nuclear translocation in endothelial cells. J. Biol. Chem. *282*, 3940–3950.

Finlan, L.E., Sproul, D., Thomson, I., Boyle, S., Kerr, E., Perry, P., Ylstra, B., Chubb, J.R., and Bickmore, W.A. (2008). Recruitment to the nuclear periphery can alter expression of genes in human cells. PLoS Genet. *4*, e1000039. http://dx.doi.org/10.1371/journal.pgen.1000039.

Glass, M., and Everett, R.D. (2013). Components of promyelocytic leukemia nuclear bodies (ND10) act cooperatively to repress herpesvirus infection. J. Virol. *87*, 2174–2185.

Imai, K., Togami, H., and Okamoto, T. (2010). Involvement of histone H3 lysine 9 (H3K9) methyltransferase G9a in the maintenance of HIV-1 latency and its reactivation by BIX01294. J. Biol. Chem. *285*, 16538–16545.

Jordan, A., Bisgrove, D., and Verdin, E. (2003). HIV reproducibly establishes a latent infection after acute infection of T cells in vitro. EMBO J. *22*, 1868–1877.

Kosak, S.T., Skok, J.A., Medina, K.L., Riblet, R., Le Beau, M.M., Fisher, A.G., and Singh, H. (2002). Subnuclear compartmentalization of immunoglobulin loci during lymphocyte development. Science *296*, 158–162.

Kumar, P.P., Bischof, O., Purbey, P.K., Notani, D., Urlaub, H., Dejean, A., and Galande, S. (2007). Functional interaction between PML and SATB1 regulates chromatin-loop architecture and transcription of the MHC class I locus. Nat. Cell Biol. *9*, 45–56.

Kuroki, M., Ariumi, Y., Ikeda, M., Dansako, H., Wakita, T., and Kato, N. (2009). Arsenic trioxide inhibits hepatitis C virus RNA replication through modulation of the glutathione redox system and oxidative stress. J. Virol. *83*, 2338–2348.

Lallemand-Breitenbach, V., and de Thé, H. (2010). PML nuclear bodies. Cold Spring Harb. Perspect. Biol. *2*, a000661.

Lo, Y.H., Wu, C.C., Shih, H.M., and Lai, M.Z. (2008). Selective activation of NFAT by promyelocytic leukemia protein. Oncogene *27*, 3821–3830.

Lusic, M., Marcello, A., Cereseto, A., and Giacca, M. (2003). Regulation of HIV-1 gene expression by histone acetylation and factor recruitment at the LTR promoter. EMBO J. *22*, 6550–6561.

Manganaro, L., Lusic, M., Gutierrez, M.I., Cereseto, A., Del Sal, G., and Giacca, M. (2010). Concerted action of cellular JNK and Pin1 restricts HIV-1 genome integration to activated CD4+ T lymphocytes. Nat. Med. *16*, 329–333.

Marcello, A., Ferrari, A., Pellegrini, V., Pegoraro, G., Lusic, M., Beltram, F., and Giacca, M. (2003). Recruitment of human cyclin T1 to nuclear bodies through direct interaction with the PML protein. EMBO J. *22*, 2156–2166.

Margolis, D.M. (2011). Eradication therapies for HIV Infection: time to begin again. AIDS Res. Hum. Retroviruses *27*, 347–353.

Miyamoto, K., Pasque, V., Jullien, J., and Gurdon, J.B. (2011). Nuclear actin polymerization is required for transcriptional reprogramming of Oct4 by oocytes. Genes Dev. *25*, 946–958.

Nayak, A., Glöckner-Pagel, J., Vaeth, M., Schumann, J.E., Buttmann, M., Bopp, T., Schmitt, E., Serfling, E., and Berberich-Siebelt, F. (2009). Sumoylation of the transcription factor NFATc1 leads to its subnuclear relocalization and interleukin-2 repression by histone deacetylase. J. Biol. Chem. *284*, 10935–10946.

Nisole, S., Stoye, J.P., and Saïb, A. (2005). TRIM family proteins: retroviral restriction and antiviral defence. Nat. Rev. Microbiol. *3*, 799–808.

Perkins, K.J., Lusic, M., Mitar, I., Giacca, M., and Proudfoot, N.J. (2008). Transcription-dependent gene looping of the HIV-1 provirus is dictated by recognition of pre-mRNA processing signals. Mol. Cell *29*, 56–68.

Rice, J.C., Briggs, S.D., Ueberheide, B., Barber, C.M., Shabanowitz, J., Hunt, D.F., Shinkai, Y., and Allis, C.D. (2003). Histone methyltransferases direct different degrees of methylation to define distinct chromatin domains. Mol. Cell *12*, 1591–1598.

Sabò, A., Lusic, M., Cereseto, A., and Giacca, M. (2008). Acetylation of conserved lysines in the catalytic core of cyclin-dependent kinase 9 inhibits kinase activity and regulates transcription. Mol. Cell. Biol. *28*, 2201–2212.

Seeler, J.S., Marchio, A., Sitterlin, D., Transy, C., and Dejean, A. (1998). Interaction of SP100 with HP1 proteins: a link between the promyelocytic leukemia-associated nuclear bodies and the chromatin compartment. Proc. Natl. Acad. Sci. USA *95*, 7316–7321.

Shalginskikh, N., Poleshko, A., Skalka, A.M., and Katz, R.A. (2013). Retroviral DNA methylation and epigenetic repression are mediated by the antiviral host protein Daxx. J. Virol. *87*, 2137–2150.

Shiels, C., Islam, S.A., Vatcheva, R., Sasieni, P., Sternberg, M.J., Freemont, P.S., and Sheer, D. (2001). PML bodies associate specifically with the MHC gene cluster in interphase nuclei. J. Cell Sci. *114*, 3705–3716.

Siliciano, R.F., and Greene, W.C. (2011). HIV latency. Cold Spring Harb Perspect Med *1*, a007096. http://dx.doi.org/10.1101/cshperspect.a007096.

Skarp, K.P., and Vartiainen, M.K. (2010). Actin on DNA-an ancient and dynamic relationship. Cytoskeleton (Hoboken) *67*, 487–495.

Solovei, I., and Cremer, M. (2010). 3D-FISH on cultured cells combined with immunostaining. Methods Mol. Biol. *659*, 117–126.

Sun, Y., Wyatt, R.T., Bigley, A., and Krontiris, T.G. (2001). Expression and replication timing patterns of wildtype and translocated BCL2 genes. Genomics *73*, 161–170.

Taddei, A., Van Houwe, G., Hediger, F., Kalck, V., Cubizolles, F., Schober, H., and Gasser, S.M. (2006). Nuclear pore association confers optimal expression levels for an inducible yeast gene. Nature *441*, 774–778.

Takizawa, T., Meaburn, K.J., and Misteli, T. (2008). The meaning of gene positioning. Cell *135*, 9–13.

Tavalai, N., and Stamminger, T. (2008). New insights into the role of the subnuclear structure ND10 for viral infection. Biochim. Biophys. Acta *1783*, 2207–2221.

Trojer, P., and Reinberg, D. (2007). Facultative heterochromatin: is there a distinctive molecular signature? Mol. Cell *28*, 1–13.

Vallian, S., Chin, K.V., and Chang, K.S. (1998). The promyelocytic leukemia protein interacts with Sp1 and inhibits its transactivation of the epidermal growth factor receptor promoter. Mol. Cell. Biol. *18*, 7147–7156.

Van Damme, E., Laukens, K., Dang, T.H., and Van Ostade, X. (2010). A manually curated network of the PML nuclear body interactome reveals an important role for PML-NBs in SUMOylation dynamics. Int. J. Biol. Sci. *6*, 51–67.

Vendrame, D., Sourisseau, M., Perrin, V., Schwartz, O., and Mammano, F. (2009). Partial inhibition of human immunodeficiency virus replication by type I interferons: impact of cell-to-cell viral transfer. J. Virol. *83*, 10527–10537.

Visa, N., and Percipalle, P. (2010). Nuclear functions of actin. Cold Spring Harb. Perspect. Biol. *2*, a000620. http://dx.doi.org/10.1101/cshperspect.a000620.

Wang, J., Shiels, C., Sasieni, P., Wu, P.J., Islam, S.A., Freemont, P.S., and Sheer, D. (2004). Promyelocytic leukemia nuclear bodies associate with transcriptionally active genomic regions. J. Cell Biol. *164*, 515–526.

Wu, W.S., Vallian, S., Seto, E., Yang, W.M., Edmondson, D., Roth, S., and Chang, K.S. (2001). The growth suppressor PML represses transcription by functionally and physically interacting with histone deacetylases. Mol. Cell. Biol. *21*, 2259–2268.

Zhang, X.W., Yan, X.J., Zhou, Z.R., Yang, F.F., Wu, Z.Y., Sun, H.B., Liang, W.X., Song, A.X., Lallemand-Breitenbach, V., Jeanne, M., et al. (2010). Arsenic trioxide controls the fate of the PML-RARalpha oncoprotein by directly binding PML. Science *328*, 240–243.

Zhao, R., Bodnar, M.S., and Spector, D.L. (2009). Nuclear neighborhoods and gene expression. Curr. Opin. Genet. Dev. *19*, 172–179.